Molecular Crystals and Liquid Crystals

Publication details, including instructions for authors and subscription information:
http://www.tandfonline.com/loi/gmcl20

Broadband Coherent Anti-Stokes Raman Scattering Microscopic Spectroscopy Using Variable-Wavelength Soliton Pulses from a Photonic Crystal Fiber

Kazuhiro Tada [a] & Naoki Karasawa [a]

[a] Department of Opto-Electronic System Engineering, Chitose Institute of Science and Technology, Chitose, Japan

Version of record first published: 25 Jun 2009

To cite this article: Kazuhiro Tada & Naoki Karasawa (2009): Broadband Coherent Anti-Stokes Raman Scattering Microscopic Spectroscopy Using Variable-Wavelength Soliton Pulses from a Photonic Crystal Fiber, Molecular Crystals and Liquid Crystals, 504:1, 181-188

To link to this article: http://dx.doi.org/10.1080/15421400902950089

Mol. Cryst. Liq. Cryst., Vol. 504, pp. 181–188, 2009
Copyright © Taylor & Francis Group, LLC
ISSN: 1542-1406 print/1563-5287 online
DOI: 10.1080/15421400902950089

Taylor & Francis
Taylor & Francis Group

Broadband Coherent Anti-Stokes Raman Scattering Microscopic Spectroscopy Using Variable-Wavelength Soliton Pulses from a Photonic Crystal Fiber

Kazuhiro Tada and Naoki Karasawa
Department of Opto-Electronic System Engineering, Chitose Institute of Science and Technology, Chitose, Japan

The object of this work is to demonstrate broadband Coherent anti-Stokes Raman scattering microscopic spectroscopy using a fundamental soliton pulse from a photonic crystal fiber as a variable-wavelength light source, where the center wavelengths of soliton pulses are controlled by a pulse shaper based on a spatial light modulator. It is demonstrated that the Raman shifts for a single 6-μm-diameter polystyrene bead were obtained for the broad range between 800 and 3100 cm^{-1} accurately. From the measurements, the three-dimensional shape of the polystyrene bead was plotted and the spatial resolutions were estimated.

Keywords: coherent anti-Stokes Raman scattering; optical soliton pulse; photonic crystal fiber

1. INTRODUCTION

Coherent anti-Stokes Raman scattering (CARS) microscopic spectroscopy is attracting attention recently. In CARS spectroscopy, a pump (angular frequency ω_1) and a Stokes (angular frequency ω_2) laser beams are used in general. When the frequency difference between theses beams ($\omega_1 - \omega_2$) coincides with the vibration frequency Ω of a sample molecule, that particular Raman vibration mode is resonantly and coherently excited. The CARS signal of $2\omega_1 - \omega_2 = \omega_{\mathrm{CARS}}$ is generated as a polarization wave when ω_1 beam interacts with the generated vibration mode by a third-order nonlinear effect. The intensity of the CARS signal is given by $I_{CARS} \propto |\chi^{(3)}|^2 I_P^2 I_S$, where $\chi^{(3)}$ is a third-order nonlinear susceptibility, I_{P} and I_{S} are the intensities of

Address correspondence to Naoki Karasawa, Department of Opto-Electronic System Engineering, Chitose Institute of Science and Technology, 758-65 Bibi, Chitose 066-8655, Japan. E-mail: n-karasa@photon.chitose.ac.jp

the incident pump and Stokes waves, respectively. The spatial resolution of CARS microscopy is expected to be high since it is a third-order nonlinear optical process. The CARS signal is not influenced by the fluorescence that can be a problem in spontaneous Raman scattering spectroscopy, because the wavelength of the CARS signal is shorter than the wavelengths of both pump and Stokes waves. The spectral resolution of a CARS signal is given by the convolution of pump and Stokes spectra. Recently, a photonic crystal fiber (PCF) is attracting attention to obtain a broadband light pulse [1]. A broadband light pulse can be obtained by propagating an optical pulse from a Ti:sapphire oscillator in a PCF. The results of CARS microscopic spectroscopy using a broadband light pulse from a PCF were reported [2–6]. We have used a fundamental soliton pulse from a PCF as a variable-wavelength Stokes pulse to observe a broadband CARS signal using a single Ti:sapphire oscillator [7]. However, the spectral range of the CARS signal was limited between 1600 and 3000 cm^{-1} and the resonant peaks of a microscopic sample were not clearly separated due to strong non-resonant background signals in the previous study.

In this study, we have improved our experimental setup such that the spectral range of CARS signals to be between 800 and 3100 cm^{-1}. Moreover, we have used a pulse shaper to shape an optical pulse before a PCF to control the center wavelength and the delay time of fundamental soliton pulses. By the use of this setup, it is possible to measure broadband CARS signals automatically and the measurements of broadband CARS signals from a single 6-µm-diameter polystyrene bead have been demonstrated. It is well known that a CARS signal usually contains resonant signals and a non-resonant signal and the dependence of the spectral intensity of the non-resonant signal on wavelength is small. However, because of the non-resonant signal, the spectral shape of the CARS signal becomes dispersive and the peak position and the amplitude of a resonant Raman signal tend to become ambiguous. We have used a nonlinear fitting program to analyze the peak amplitude of the particular Raman signal of a sample. Here, the peak amplitude of a Raman signal near 1000 cm^{-1} has been used to obtain the three-dimensional shape of a 6-µm-diameter polystyrene bead and the spatial resolution of the measurement has been estimated.

2. EXPERIMENTAL METHODS

Experimental setup is shown in Figure 1. A pulse from a Ti:sapphire laser oscillator (center wavelength 810 nm, pulse width 50 fs, average

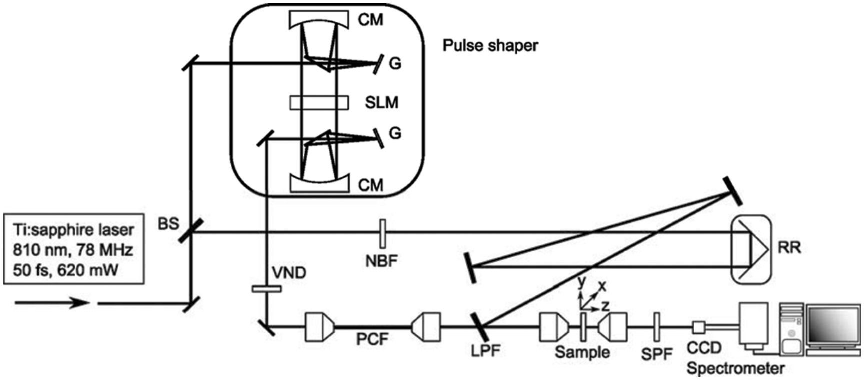

FIGURE 1 Experimental setup of a CARS microscopic spectroscopy: BS, beam splitter; RR, retroreflector; VND, variable neutral density filter; NBF, narrow-bandpass filter (808 nm); DM, dichroic mirror; LPF, long-pass filter (840 nm); SPF, short-pass filters (785 and 850 nm); CM, concave mirror (203 mm focal length); G, grating (1200 grooves/mm).

power 620 mW, and repetition rate 78 MHz) was split into two pulses by a beam splitter and one of the pulse was used as a pump pulse after its spectrum was narrowed by a band pass filter (center wavelength 808 nm with a 3-nm full width at half maximum bandwidth). The other pulse was used as a Stokes pulse after it was shaped by a pulse shaper and was propagated in a 120-mm-long PCF (Crystal Fibre NL-1.5-590) to generate a fundamental soliton pulse. A long-pass filter was used to eliminate the shorter-wavelength components than soliton's wavelength. Both pulses were overlapped collinearly and focused on a sample using an objective (100X, 0.9 numerical aperture). The average input powers on a sample were about 9 mW for a pump beam and about 5 mW for a Stokes beam. The signal from the sample was collected by an objective and was detected by a spectrometer (Solar TII MS-3504) with a CCD detector (Andor DV420-OE) after the spectral components of both pump and Stokes pulses were removed by the use of short-pass filters. Initially, the center wavelength of a soliton pulse from a PCF was set to be 1050 nm (which corresponds to vibration frequency 3000 cm^{-1}) by adjusting the power of an input pulse. The center wavelength of a soliton pulse was shifted to shorter wavelength by applying a phase pattern by a spatial light modulator (SLM; JenOptik SLM-S320) in a pulse shaper. The pulse shaper consists of the SLM, two pairs of gratings, concave mirrors, and folding mirrors. In experiment, six different cosine phase patterns were used such that the spectra of soliton pulses covered the wavelength between 850 and 1050 nm uniformly. The cosine phase pattern is given by $A \cos \omega T$ and when this phase pattern was used, the pulse train of an original pulse was created with a period T and the peak amplitude of the central pulse was determined by the Bessel function of zero order $J_0(A)$ [8]. The period T was set to be 500 fs in experiment such that the timing of only the central pulse in a pulse train matched with a pump pulse. The phase pattern of a form $\beta_1(\omega-\omega_0)$ was added to control the delay time of an input pulse with respect to a pump pulse, where β_1 is the group delay and ω_0 is the center angular frequency of a pump pulse. In Figure 2, the spectra of soliton pulses with six different center wavelengths are shown. As shown in this figure, by using six soliton pulses with different center wavelengths, the spectral regions between 850 and 1050 nm were covered almost uniformly. The exposure time to obtain CARS signals was set to be 0.5 second for each soliton pulse with a different wavelength, thus the total exposure time to obtain CARS signals between 800 and 3100 cm^{-1} was 3 seconds. In addition to this, the switching time of the phase pattern in a SLM was required (about 0.4 second for every switching). The measurements of CARS signals were performed as the sample position was changed by a three-axis motorized stage.

The CARS signal contains both resonant and non-resonant contributions and usually only the resonant contributions are important since the wavelength dependence of non-resonant signal is small. To extract the resonant contribution from the CARS signal, the

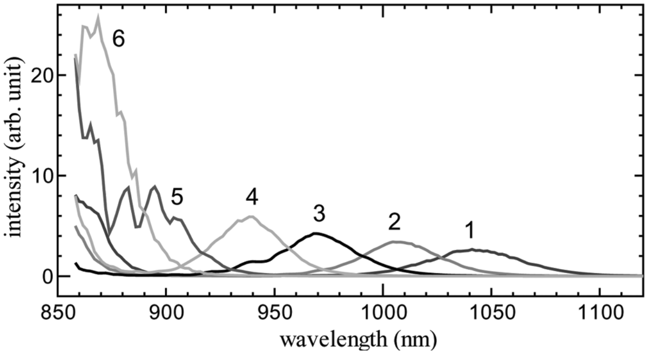

FIGURE 2 The spectra of soliton pulses for different phase patterns, where the phase pattern is given by $\varphi(\omega) = \beta_1(\omega-\omega_0) + A\cos\omega\mathrm{T}$, 1: $\beta_1 = -350$ fs, $A = 0$, 2: $\beta_1 = -200$ fs, $A = 0.5$, 3: $\beta_1 = -50$ fs, $A = 0.75$, 4: $\beta_1 = 10$ fs, $A = 1.1$, 5: $\beta_1 = 50$ fs, $A = 1.2$, and 6: $\beta_1 = 200$ fs, $A = 1.3$.

signal from a glass substrate was measured independently and it was used as a non-resonant signal and the signal from a sample was normalized by this signal. After this procedure, the CARS signal can be written [9] as

$$I_{CARS}(\omega) = \left| a + \sum_{j=1}^{n} \frac{R_j}{\Omega_j - \omega + i\Gamma_j} \right|^2, \tag{1}$$

where ω is an angular frequency, R_j, Ω_j, and Γ_j are the amplitude, angular frequency and width parameters of jth Raman vibration mode, and a is a parameter to show the relative intensity of a non-resonant signal and a resonant signal. To accurately evaluate the shape of a sample in a microscopy setup, we have fitted CARS signals at different sample positions using Eq. (1) to obtain the amplitude parameter R_{j} and plotted this value as a function of the position of the sample. For the fitting, nonlinear fitting program based on Levenberg-Marquard method was used [10]. For a polystyrene bead sample, only a single Raman vibration mode near 1000 cm^{-1} was used for the fitting and its amplitude parameter was used to plot the shape of the sample.

3. RESULTS AND DISCUSSION

The result of CARS spectroscopy of a single 6-μm-diameter polystyrene bead is shown in Figure 3. A signal from the sample using a pump pulse and six Stokes pulses in Figure 2 was measured where the wavelengths of Stokes pulses were controlled by the cosine phase patterns

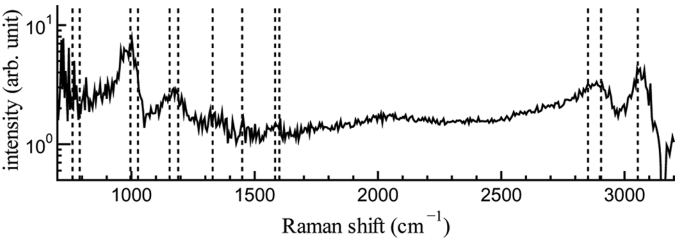

FIGURE 3 The normalized CARS signal of a single 6-μm-diameter polystyrene bead sample, where the wavelength of a soliton was controlled by cosine phase patterns. The Raman peak positions obtained by spontaneous Raman spectroscopy are indicated by dotted lines.

applied by the SLM. The signal was normalized by the non-resonant signal obtained independently from a glass substrate. The known Raman peaks (Fig. 3, dotted lines) obtained from spontaneous Raman spectroscopy were observed clearly in CARS signals between 800 and 3100 cm^{-1}. The spectral widths of Raman peaks were determined by the spectral width of a pump pulse and in our setup, the spectral resolution was about 50 cm^{-1}.

The CARS microscopic images of the same polystyrene bead are shown in Figure 4. Figure 4(a) is a CARS microscopic spectroscopy image of a polystyrene bead at Raman shift near 1000 cm^{-1}. 100 CARS signals were obtained as the sample was moved perpendicular to the optical axis every 1 μm step for X and Y directions to obtain this image and the Raman amplitudes near 1000 cm^{-1} were extracted by the nonlinear fitting program for this plot. Figure 4(b) is a CARS microscopic

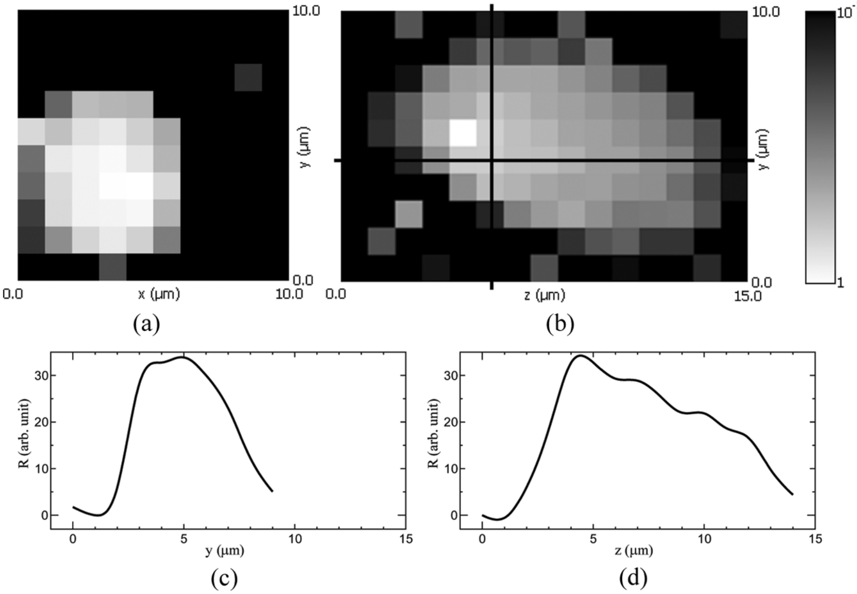

(a) (b)

(c) (d)

FIGURE 4 The CARS microscopic image of a single 6-μm-diameter polystyrene bead in the direction perpendicular to the optical axis (a) and in the direction parallel to the optical axis (b) using the fitted Raman amplitude parameter R. In (c), the Raman amplitude parameter R is plotted as function of Y position where the position is indicated by a vertical line in (b). In (d), the R parameter is shown as function of Z position where the position is indicated by a horizontal line in (d).

spectroscopy image of a polystyrene bead at the same Raman shift when the sample was moved in Y and Z directions, where Z direction corresponds to the optical axis. In this case, 150 CARS signals were measured. In Figure 4(c), the variation of fitted Raman amplitude parameter R is shown as a function of Y position. The movement of a sample in this case is perpendicular to the optical axis and is indicated by a vertical line in Figure 4(b). In Figure 4(d), the variation of fitted Raman amplitude parameter R is shown similarly as a function of Z position. The movement of a sample in this case is parallel to the optical axis and the left side corresponds to the interface between the air and the polystyrene bead and the right side corresponds to the interface between the glass substrate and the polystyrene bead. From Figure 4(c), we have estimated the spatial resolution in the perpendicular direction to be about 2.7 μm by taking the derivative of R parameter and measuring the width of a peak near $Y = 2.5\,\mu m$. From Figure 4(d), we have estimated the spatial resolution in the parallel direction to be about 2.7 μm for the interface between the air and the polystyrene bead by using the similar procedure.

4. CONCLUSION

In this study, it is demonstrated that the broadband Raman shift between $800\,cm^{-1}$ and $3100\,cm^{-1}$ for a single 6-μm-diameter polystyrene bead can be detected and the CARS microscopic images can be obtained by using a fundamental soliton pulse as a variable-wavelength light source, where its wavelength is controlled by a pulse shaper using the SLM. To extract the resonant contribution from CARS signals, a nonlinear fitting program was used to obtain the Raman amplitude parameter and this parameter was used to plot the three-dimensional shape of the polystyrene bead sample and to estimate the spatial resolutions. The spatial resolution of CARS measurement was found to be about 2.7 μm for both in the perpendicular direction and in the parallel direction to the optical axis.

REFERENCES

[1] Russell, P. St. J. (2003). *Science*, *299*, 358–362.

[2] Paulsen, H. N., Hilligsoe, K. M., Thogersen, J., Keiding, S. R., & Larsen, J. J. (2003). *Opt. Lett.*, *28*, 1123–1125.

[3] Kee, T. W. & Cicerone, M. T. (2004). *Opt. Lett.*, *29*, 2701–2703.

[4] Kano, H. & Hamaguchi, H. (2005). *Appl. Phys.*, *86*, 121113.

[5] Kano, H. & Hamaguchi, H. (2006). *J. Raman Spectrosc.*, *37*, 411–415.

[6] Andresen, E. R., Birkedal, V., Thogersen, J., & Keiding, S. R. (2006). *Opt. Lett.*, *31*, 1328–1330.

[7] Tada, K. & Karasawa, N. (2008). Coherent anti-stokes Raman scattering microspectroscopy using a fundamental soliton pulse generated from a photonic crystal fiber. In: *Optical Materials and Devices New Stage*, Tanio, N. & Sasabe, H. (Eds.), PWC Publishing: Chitose, Japan, 215–220.

[8] Morita, R. & Toda, Y. (2005). Field manipulation of ultra broadband optical pulses. In: *Mono-Cycle Photonics and Optical Scanning Tunneling Microscopy*, Yamashita, M., Shigekawa, H., & Morita, R. (Eds.), Springer: Berlin, 251–283.

[9] Wurpel, G. W. H., Schins, J. M., & Müller, M. (2002). *Opt. Lett.*, *27*, 1093–1095.

[10] Press, W. H., Flannery, B. P., Teukolsky, S. A., & Vetterling, W. T. (1988). *Numerical Recipes in C*, Cambridge University Press: Cambridge, UK.